

# Multiferroic properties of $\text{Pb}(\text{Zr}, \text{Ti})\text{O}_3/\text{CoFe}_2\text{O}_4$ composite thin films

N. Ortega,<sup>a)</sup> P. Bhattacharya, and R. S. Katiyar<sup>b)</sup>

*Department of Physics, University of Puerto Rico, San Juan 00931-3343, Puerto Rico*

P. Dutta, A. Manivannan, and M. S. Seehra

*Department of Physics, West Virginia University, Morgantown, West Virginia 26506*

I. Takeuchi

*Small Smart Systems Center, Department of Materials Science and Engineering, University of Maryland, College Park, Maryland 20742*

S. B. Majumder

*Materials Science Center, Indian Institute of Technology, Kharagpur 721 302, India*

(Received 16 August 2006; accepted 30 September 2006; published online 26 December 2006)

In the present work we report multiferroic behavior in lead zirconate titanate (PZT)–cobalt iron oxide (CFO) composite thin films. It is found that upon annealing, the multilayered structures are intermixed at least partially, and CFO is phase separated into PZT matrix to form a composite film. The phase separation behavior has been characterized by x-ray photoelectron spectroscopy depth profiling of the constituent elements in conjunction with dielectric spectroscopy measurements. The composite films exhibited ferroelectric as well as ferromagnetic characteristics at room temperature. The coupling between the ferroelectric and the ferromagnetic order parameters has been demonstrated through the reduction of ferroelectric polarization when measured under an applied magnetic field. © 2006 American Institute of Physics. [DOI: [10.1063/1.2400795](https://doi.org/10.1063/1.2400795)]

In recent years, there has been an increasing interest in multiferroic materials due to their potential applications.<sup>1</sup> The available single-phase materials have lower magnetoelectric coefficients for possible devices applications.<sup>2,3</sup> It has been proposed recently to achieve such a coupling by designing composites with magnetostrictive and piezoelectric phases via a stress mediation.<sup>4,5</sup> Further research efforts were directed to synthesize composite thin films which included a composition spread with terminal layers being ferromagnetic and ferroelectric,<sup>6</sup> layer-by-layer growth,<sup>7</sup> superlattices,<sup>8</sup> as well as epitaxial growth of ferromagnetic and ferroelectric layers on suitable substrates.<sup>9</sup> Through these studies it has emerged that the distribution as well as orientation of the magnetostrictive phase in piezoelectric matrix affect significantly the magnetoelectric coupling of the composite multiferroic thin films. It was claimed that since the magnetoelectric coupling is through elastic interaction, in the multilayered structures, due to the clamping effect of the substrate, any such effect will be negligible.<sup>9,10</sup> Contrary to all these reports, recently the magnetoelectric (ME) behavior has been demonstrated in sol-gel deposited  $\text{CoFe}_2\text{O}_4$ – $\text{Pb}(\text{Zr}, \text{Ti})\text{O}_3$  multilayered films,<sup>11</sup> although through these studies, the factor(s) responsible for the occurrence of ME behavior in these films has (have) not been delineated.

In the present work, we have synthesized multilayered  $\text{Pb}(\text{Zr}_{0.53}\text{Ti}_{0.47})\text{O}_3$  (PZT)– $\text{CoFe}_2\text{O}_4$  (CFO) thin films on platinumized silicon substrate using pulsed laser deposition. It was observed that the thickness of the individual PZT as well as

CFO layers, annealing temperature, and time could be optimized to yield phase-separated CFO grains in PZT matrix. In other words, the as-deposited 2-2 (layer-by-layer)-type composite films were converted into 0-3 (CFO phase separated into PZT matrix)-type composite film under optimized conditions. The composite films exhibit room temperature ferroelectric, ferromagnetic hysteresis loops and the desired magnetoelectric coupling.

Using pulsed laser deposition, the substrate was coated by alternate deposition of PZT and CFO layers to attain a multilayered 350 nm film, having the following configuration: substrate/PZT(90 nm)/CFO(40 nm)/PZT(90 nm)/CFO(40 nm)/PZT(90 nm). The substrate temperature and the oxygen partial pressure in the deposition chamber were maintained to be 400 °C and 100 mTorr, respectively. The as-deposited films were postannealed using a rapid thermal annealing (RTA) furnace at temperatures ranging from 650 to 750 °C for 150 s. An x-ray diffractometer (XRD) was used to characterize the phase formation behavior of the annealed films. The depth profile of the constituent elements of the multilayered films was studied using x-ray photoelectron spectroscopy (XPS). The dielectric properties of the films were measured using an impedance analyzer, whereas an automated hysteresis loop tracer was utilized to measure the ferroelectric characteristics of the annealed films after platinum (circular with diameter of 200  $\mu\text{m}$ ) top electrode deposition. The magnetic properties of the multilayered films were measured using a superconducting quantum interference device (SQUID) magnetometer.

From a comparison of the XRD patterns of a five-layered PZT–CFO multilayered film (not shown) and pure PZT and CFO films, grown at same conditions, it was concluded that all the peaks corresponding to the PZT and CFO

<sup>a)</sup>Electronic mail: [norapatria50@gmail.com](mailto:norapatria50@gmail.com)

<sup>b)</sup>Author to whom correspondence should be addressed; FAX: 787-764-2571; electronic mail: [rkatiyar@uprrp.edu](mailto:rkatiyar@uprrp.edu)

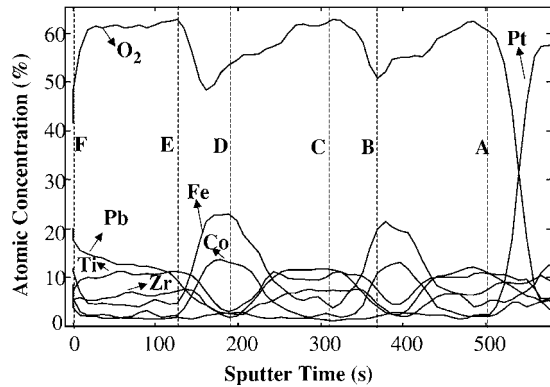


FIG. 1. XPS depth profile graph of the constituent elements of PZT-CFO thin films, the drawn vertical lines indicate the tentative position of PZT/CFO interface (B and D), CFO/PZT (C and E), the substrate and PZT interface (A), and PZT and air interfaces (F).

phases are present in the multilayered film without the appearance of any additional peak(s). These observations suggest that the individual piezoelectric as well as magnetostrictive phases are retained in the multilayered films. We have performed XPS depth profilometry to determine the atomic contents of Co, Fe, Pb, Zr, Ti, as well as Pt and O ions in the PZT-CFO multilayered thin films; the percentage concentration of each element was acquired from XPS signal area divided by the corresponding atomic sensitivity factor (ASF), and the results are presented in Fig. 1. Assuming that the sputtering rate (calibrated to be  $\sim 7 \text{ \AA s}^{-1}$ ) is identical both for PZT as well as CFO layers, the drawn vertical lines indicate the tentative position for substrate-PZT (layer 1) (marked A), PZT (layer 1)-CFO(layer 1) (marked B), CFO (layer 1)-PZT (layer 2) (marked C), PZT (layer 2)-PZT (layer 3) (marked E), and finally PZT (layer 3) and air (marked F) interfaces for five-layered PZT-CFO multilayered films. Figure 1 clearly shows that the individual CFO and PZT layers are intermixed and the as-deposited layered structure is not maintained. From several literature reports, it is known that there exists very little solid solubility between the spinel and perovskite phases.<sup>9-12</sup> However, the key point here to note is that the annealing condition was sufficient to obtain mixing between two layers; however, XPS shows that there exist alternate layers, rich in CFO and PZT. Similar observations have also been reported in other material system and a thermodynamic instability hypothesis has been invoked to explain the observed behavior.<sup>13</sup> The ratio of  $[\text{Pb}]:[\text{Zr}+\text{Ti}]$  and  $[\text{Co}]:[\text{Ti}]$  was estimated at various points within each of the five individual layers and the average compositions were found to be  $\sim 0.77$  and  $0.49$ , respectively. The significant lead deficiency is assumed to be due to the higher sputtering yield of lead. However, the fact that even in the PZT layer, the  $[\text{Co}]:[\text{Fe}]$  ratio is maintained to be close to  $0.5:1$ , the assumption of intermixing among the individual CFO and PZT layer is justified. The XPS depth profile analyses indicate that the as-deposited 2-2-type composite thin film, upon rapid thermal annealing, forms a 0-3-type composite film.

Figure 2 shows the frequency dispersion (1 kHz–1 MHz) of (a) the dielectric constant ( $k$ ) and (b) the loss tangent ( $\tan \delta$ ) of the composite film in the temperature

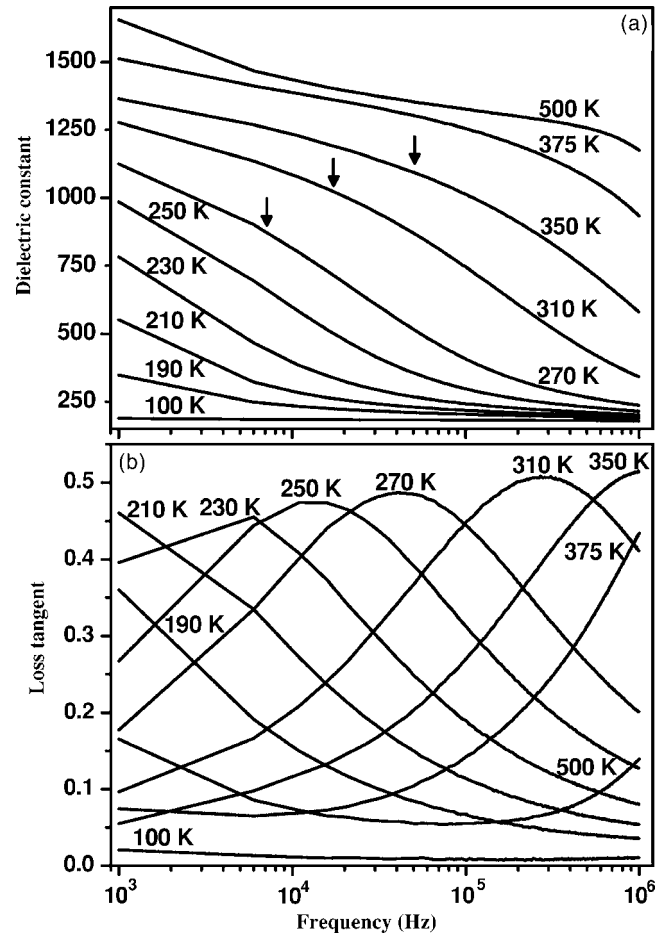


FIG. 2. Frequency dispersion of (a) the dielectric constant and (b) loss tangent of PZT-CFO thin films.

range of 100–500 K. As shown in Fig. 2(a), a marginal dielectric dispersion is observed over a wide frequency range (first plateau) ( $\sim 10 \text{ kHz}$ – $300 \text{ kHz}$ ) at temperatures  $\geq 375 \text{ K}$ . As the temperature is reduced ( $\approx 300 \text{ K}$ ), the dielectric dispersion is more pronounced and the dielectric constant reduces more rapidly beyond an onset frequency (marked by a small arrow). The onset frequency is progressively lowered with the reduction in temperature. Finally on further cooling, ( $\approx 200 \text{ K}$ ), a second plateau is identified.

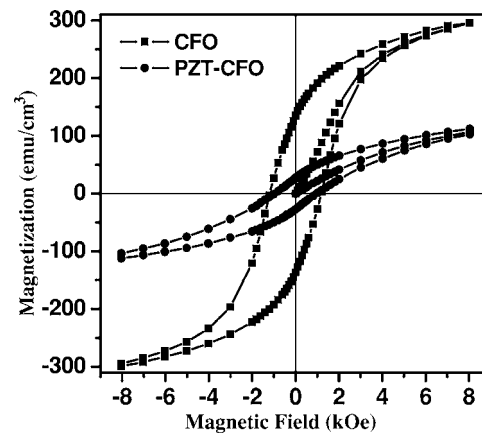


FIG. 3. Ferromagnetic hysteresis loops of CFO and PZT-CFO thin films measured at room temperature.

The relaxation of the  $k$  dielectric constant is also accompanied by a loss peak, which shifts to higher frequency with the increase in temperature. The temperature dependent  $k$  and  $\tan \delta$  (not shown) exhibit the following features: (i) almost temperature independent dielectric constant at elevated temperature followed by a steplike decrease at relatively lower temperature, (ii) the temperature corresponding to the initiation of the rapid fall of the measured  $k$  shifts to higher temperature with the increase in frequency, and (iii) the steplike decrease of the  $k$  also associated with a peak in the  $\tan \delta$  values, and the  $\tan \delta$  peak shifts to higher temperature with the increase in the frequency. These observations are similar to those reported for materials exhibiting colossal dielectric constant (CDC) behavior.<sup>14,15</sup> Such behavior is electrically equivalent to two parallel-connected resistor-capacitor (RC) circuits connected in series. Each RC element gives rise to a plateau in the spectroscopic plot of the real component of the dielectric constant. Within the window of the measured frequency (1 kHz–1 MHz), depending on the measurement temperature, we could observe the two plateaus, which are thought to be due to the CFO and PZT regions, respectively. The high values of the  $k$  over a wide temperature range are thought to be due to Maxwell-Wagner-type contributions of depletion layers at the interface between PZT and CFO phase-separated regions.<sup>14</sup>

The composite film exhibits ferroelectric as well as ferromagnetic hysteresis loops at room temperature. PZT–CFO composite film shows well-defined ferroelectric loop with remnant polarization ( $P_r$ ) and coercive fields ( $E_c$ ) of about  $25 \mu\text{C cm}^{-2}$  and  $68 \text{ kV cm}^{-1}$ , respectively. The  $P_r$  and  $E_c$  for pure PZT thin film have been measured to be  $33 \mu\text{C cm}^{-2}$  and  $37 \text{ kV cm}^{-1}$ , respectively. The dilution of the  $P_r$  value of the composite film is expected to be due to the presence of nonferroelectric CFO region, which also hinders the domain wall motion of the ferroelectric region to increase the  $E_c$  in the composite film. As shown in Fig. 3, the saturation magnetization ( $M_s$ ) of CFO ( $\sim 350 \text{ emu cm}^{-3}$ ) is twice that measured for PZT–CFO composite thin films ( $\sim 166 \text{ emu cm}^{-3}$ ). The magnitudes of the remnant magnetization ( $M_r$ ) and coercive field ( $H_c$ ) for CFO and PZT–CFO composite thin films are measured to be  $135 \text{ emu cm}^{-3}$  and  $1.18 \text{ kOe}$  and  $26 \text{ emu cm}^{-3}$  and  $0.96 \text{ kOe}$ , respectively. The magnitudes of  $M_s$  and  $M_r$  measured for pure CFO film are similar to those reported for bulk CFO measured at 300 K ( $M_s \sim 350 \text{ emu cm}^{-3}$ ,  $M_r \sim 150 \text{ emu cm}^{-3}$ ).<sup>16</sup> The coupling between the ferroelectric and ferromagnetic orderings is demonstrated through the measurement of polarization hysteresis in the presence of magnetic field (Fig. 4). Both the saturation as well as remnant polarization values were reduced with the increase in magnetic field. Similar observations have been reported in the case of multiferroic  $\text{Bi}_{0.6}\text{Tb}_{0.3}\text{La}_{0.1}\text{FeO}_3$  thin films and the observed behavior has been related to the magnetic field induced disturbance in the grain alignment.<sup>17</sup> Kimura *et al.* also reported that in  $\text{TbMnO}_3$  the polarization was found to decrease along the  $c$  axis with the increase in magnetic field.<sup>18</sup>

In summary, we have synthesized composite PZT–CFO thin films on platinized silicon substrate using pulsed laser deposition with a thickness of  $\sim 350 \text{ nm}$ . Upon rapid thermal

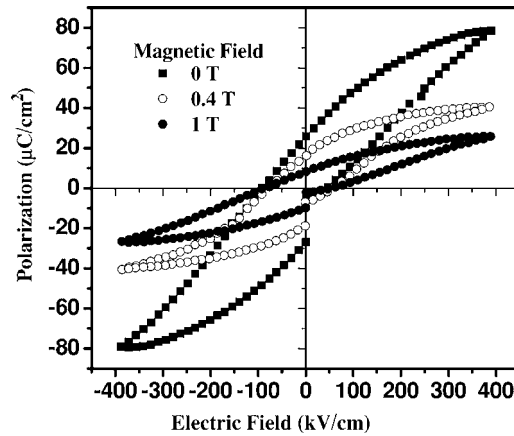


FIG. 4. Polarization hysteresis of PZT–CFO thin films measured applying magnetic field in the range of 0–1 T.

annealing, it was found that the layer-by-layer structure of PZT and CFO was mixing and CFO was phase separated into the PZT matrix. The formation of such phase-separated region has been confirmed by XPS depth profile in conjunction with dielectric spectroscopy analyses. The PZT–CFO composite thin film had a room temperature  $k$  and of 750 and 0.45, respectively (at 100 kHz). The films also exhibited both magnetization and polarization hysteresis at room temperature. The multiferroic nature of the composite is demonstrated through the reduction of measured ferroelectric polarization with the application of external magnetic field.

The work at the University of Puerto Rico was supported in part by DoD-W911NF-06-1-0030 and W911NF-06-1-0183 grants.

<sup>1</sup>N. A. Spaldin and M. Fiebig, *Science* **309**, 391 (2005).

<sup>2</sup>M. Fiebig, *J. Phys. D* **38**, R123 (2005).

<sup>3</sup>W. Prellier, M. P. Singh, and P. Murugavel, *J. Phys.: Condens. Matter* **17**, R803 (2005).

<sup>4</sup>J. Zhai, N. Cai, Z. Shi, Y. Lin, and C. W. Nan, *J. Appl. Phys.* **95**, 5685 (2004).

<sup>5</sup>J. Ryu, A. Vázquez, K. Uchino, and H. E. Kim, *J. Electroceram.* **7**, 17 (2001).

<sup>6</sup>K. S. Chang *et al.*, *Appl. Phys. Lett.* **84**, 3091 (2004).

<sup>7</sup>J. P. Zhou, H. He, Z. Shi, and C. W. Nan, *Appl. Phys. Lett.* **88**, 013111 (2006).

<sup>8</sup>P. Murugavel, M. P. Singh, W. Prellier, B. Mercey, Ch. Simon, and B. Raveau, *J. Appl. Phys.* **97**, 103914 (2005).

<sup>9</sup>H. Zheng *et al.*, *Science* **303**, 661 (2004).

<sup>10</sup>C. W. Nan, G. Liu, Y. Lin, and H. Chen, *Phys. Rev. Lett.* **94**, 197203 (2005).

<sup>11</sup>J. G. Wan *et al.*, *Appl. Phys. Lett.* **86**, 122501 (2005).

<sup>12</sup>J. P. Zhou, H. He, Z. Shi, and C. W. Nan, *Appl. Phys. Lett.* **88**, 013111 (2006).

<sup>13</sup>M. Meixner, E. Scholl, V. A. Shchukin, and D. Bimberg, *Phys. Rev. Lett.* **87**, 236101 (2001).

<sup>14</sup>P. Lunkenheimer, V. Bobnar, A. V. Pronin, A. I. Ritus, A. A. Volkov, and A. Loidl, *Phys. Rev. B* **66**, 052105 (2002); P. Lunkenheimer, R. Fichtl, S. G. Ebbinghaus, and A. Loidl, *ibid.* **70**, 172102 (2004).

<sup>15</sup>L. Feng, X. Tang, Y. Yan, X. Chen, Z. Jiao, and G. Cao, *Phys. Status Solidi A* **203**, R22 (2006).

<sup>16</sup>A. Manivannan, A. M. Constantinescu, and M. S. Seehra, *Mater. Res. Soc. Symp. Proc.* **658**, GG6.32.1 (2001).

<sup>17</sup>V. R. Palkar, K. G. Kumara, and S. K. Malik, *Appl. Phys. Lett.* **84**, 2856 (2004).

<sup>18</sup>T. Kimura, T. Goto, H. Shintani, K. Ishizaka, T. Arima, and Y. Tokura, *Nature (London)* **426**, 55 (2003).